applied sciences

MDPI

Article

Novel Phenotypic Elements of Type IV Collagenopathy Revealed by the *Drosophila* Model

András A. Kiss [1], Nikoletta Somlyai-Popovics [1], Vilmos Tubak [2], Zsolt Boldogkői [1], Katalin Csiszár [3] and Mátyás Mink [1,*]

1 Institute of Medical Biology, University of Szeged, H-6720 Szeged, Hungary; kiss.andras.attila@med.u-szeged.hu (A.A.K.); somlyai-popovics.nikoletta@med.u-szeged.hu (N.S.-P.); boldogkoi.zsolt@med.u-szeged.hu (Z.B.)
2 Creative Laboratory Ltd., H-6726 Szeged, Hungary, tubak.vilmos@brc.mta.hu
3 John A. Burns School of Medicine, University of Hawaii, Honolulu, HI 96822, USA; katalin@hawaiii.edu
* Correspondence: mink@bio.u-szeged.hu

Received: 5 April 2019; Accepted: 13 May 2019; Published: 21 May 2019

Featured Application: A great number of drugs can be screened with the aid of the high-throughput *Drosophila* system to combat type IV collagenopathy.

Abstract: Type IV collagen is proposed to be a key molecule in the evolvement of multicellular animals by forming the architectural unit basement membrane, a specialized form of the extracellular matrix. Functions of the basement membrane include guiding organ regeneration, tissue repair, modulation of cell differentiation, apical–basal polarity identification, cell migration and adhesion, regulation of growth factor signaling gradients, maintenance of tissue architecture and compartmentalization. Type IV collagenopathy is a devastating systemic disease affecting the circulatory, renal and visual systems and the skeletal muscles. It is observed in patients carrying mutations in the *COL4A1* gene, which codes for the ubiquitous basement membrane component. *Col4a1* mouse mutants display the human symptoms of type IV collagenopathy. We chose the *Drosophila melanogaster* model as we recorded dominant, temperature-sensitive mutations in the cognate *col4a1* gene of the fruit fly and demonstrated phenotypic elements which have not yet been explored in humans or in mouse models. In this paper we show a transition of the Z-discs, normally bordering each sarcomere, to the level of M-discs significantly penetrant in the mutants, uneven distribution of fused mitochondria in the Malpighian tubules of the excretory organ and a loss of sarcomere structure in the visceral muscles in the gut of mutants. Our observations demonstrate the systemic nature of the *col4a1* mutations in the fruit fly. However, these traits are elements of the type IV collagen-associated pathology and may provide insights into approaches that can alleviate symptoms of the disease.

Keywords: type IV collagen; mutation; multisystem disease; *Drosophila* model

1. Introduction

The highly differentiated form of the extracellular matrix is the planar-organized basement membrane (BM) found at the basal side of epithelial and endothelial cells in neural, vascular and adipose tissues, surrounding each individual striated muscle fiber.

Major proteins of BMs are type IV collagen, laminin, nidogen or entactin, perlecan and integrins [1]. Nidogens and perlecan are required perinatally but not at earlier phases of development [2]. The BM is anchored to the cell-surface integrin and to the dystroglycan receptors and provides a BM–cytoskeleton linkage [3]. The family of laminins consists of five alpha, four beta and three gamma chains in mammals. They harbor three pairs of type IV collagen genes, *COL4A1* through to *COL4A6*, with each gene pair

in head-to-head genomic organization [4–6]. Defects in BM components are often linked to human genetic diseases. An example of a laminin disorder is Lma2, merosin-deficient congenital muscular dystrophy (MDC1A and limb-girdle type) arising from lesions in the *LAMA2* gene, it affects skeletal muscles and the neural system [7,8]. Mutations of the *LAMB2* gene cause Pierson syndrome, a form of focal segmental glomerulosclerosis [9].

Nearly 100 years ago, A.C. Alport reported about "hereditary familial congenital hemorrhagic nephritis" predominantly affecting men [10]. Type IV collagen genes were isolated many decades later, starting with *COL4A1* [11], which was placed at the tip of the long arm of chromosome 13 [12]. Discovery of the rest of the five type IV collagen genes soon followed [13–17]. Association of the *COL4A5* gene mutations was demonstrated in patients with X-chromosomal Alport syndrome [18,19]. Alport syndrome has a digenic inheritance. Only 80% of the patients carried mutations in the X-chromosomal *COL4A5* gene, whereas the rest had lesions in the autosomal *COL4A3* locus at 2q36.3 [20,21]. The glomerular capillaries filter plasma through the glomerular basement membrane consisting of COL4A3, COL4A4 and COL4A5 heterotrimers. This isoform is absent from the glomeruli in patients with X-linked Alport syndrome and that harbor the fetal $(COL4A1)_2COL4A2$ trimers, with increased susceptibility to proteolytic attack by collagenases and cathepsins [22,23].

We identified dominant, temperature-sensitive mutations in the *Drosophila* type IV collagen gene *col4a1* exclusively. The *col4a1* $^{+/-}$ heterozygotes are viable and fertile at 20 °C, the permissive temperature; however, they perish under the restrictive condition, 29 °C. The dominant-negative, antimorphic phenotype suggests the incorporation of mutant COL4A1 monomers into the planar-organized triple helices. The genome of the fruit fly consists of a pair of type IV collagen genes, *col4a1* and *col4a2* in a head-to-head orientation, similar to mammals [24]. The mutant phenotype is systemic, affecting the gut [25,26], the excretory organ Malpighian tubules [27,28] and the muscles manifested in muscular dystrophy [29]. The recessive phenotype of the *col4a1* $^{-/-}$ homozygotes leads to lethality in the late embryonic to early larval phases at the permissive temperature [24]. Type IV collagen in *Drosophila* appears to fulfill a similar function as in mammals by providing BM stiffness and elasticity. Beyond conserved genomic organization, both genes and proteins share a high level of identity and similarity [24].

The clinical spectrum of *COL4A1*-associated defects is wide. Pedigrees of families in the Netherlands were identified as presenting cerebral porencephaly [30]. Mapping placed autosomal dominant type 1 porencephaly at the tip of chromosome arm 13q [31]. These families were assessed for mutations in the *COL4A1* gene and missense Gly substitutions were demonstrated within the gly-X-Y repeats in the $(COL4A1)_2COL4A2$ triple helical domain [32]. Three families were diagnosed with autosomal dominant hereditary angiopathy with nephropathy, aneurysms and muscle cramps (HANAC) [33]. Sequencing revealed three close glycine mutations in the highly conserved exons 24 and 25 of the *COL4A1* gene, affecting the integrin-binding site within the COL4A1 protein. Within the three families recapitulating the key features of HANAC, three different heterozygous missense mutations in the *COL4A1* gene were demonstrated [34]. In a Spanish family with tortuosity of the retinal arteries, retinal hemorrhage was identified [35]. Interestingly, the lesion was not associated with muscle cramps, renal or brain anomalies, although the p.G510R mutation was previously detected in a French family with HANAC syndrome [34]. The different apparent expressivity of the associated trait was explained by environmental factors or genetic modifiers that may influence the phenotypic manifestation and the extent of organ involvement in *COL4A1*-related disease. In a study on the susceptibility to intracerebral hemorrhage, in two of 96 unrelated patients with adult-onset hemorrhagic stroke, the p.P352L substitution at the highly conserved Y-position of a gly-X-Y repeat and the p.R538G replacement were identified within the *COL4A1* gene [36]. Heterozygosity for a missense mutation in the *COL4A1* gene was identified in a boy with schizencephaly, renovascular hypertension, retinal arteriosclerosis and alveolar hemorrhage [37,38]. In 183 mostly pediatric patients with cerebral hemorrhage or porencephaly, 21 *COL4A1* and three *COL4A2* mutations were identified at a 40% sporadic mutation rate [39]. Diagnosis in some patients with *COL4A1* mutations were consistent

with Walker–Warburg Syndrome or muscle–eye–brain disease, a distinct form of congenital muscular dystrophy [40].

Mouse *Col4a1* mutants recapitulate human disease. An allelic series of induced dominant mouse mutants was identified and showed ocular anterior segment defects or Axenfeld–Rieger anomaly, vacuolar cataracts, corneal opacities, iris defects, iris or corneal adhesions, buphthalmos, optic nerve cupping, retinal detachment and developed renal glomerulopathy [41]. Similar ophthalmic defects were noted in the *Col4a1* splice site of mutant C57BL6/J mice. When C57BL6/J mice were crossed with 129/SvEvTac and CAST/EiJ inbred strains, the F1 progeny were phenotypically almost indistinguishable from the wild-type. Genetic mapping identified a co-segregating dominant locus on chromosome 1, that likely contains the suppressor and modifier genes [42]. *Col4a1*$^{G498V/G498V}$ homozygous mice showed severe muscular dystrophy, including muscle mass decrease, fiber atrophy, centronuclear fibers, fibrosis, focal perivascular inflammation and intramuscular hemorrhaging [43]. Variants closer to the C-terminus tended to result in increased intracellular levels of the Col4a1 protein, whereas those closer to the N-terminus tended to accumulate lower amounts of intracellular proteins with unchanged clinical severity [44]. The renal manifestation in mouse models of HANAC syndrome include albuminuria, hematuria, glomerular cysts and delays in glomerulogenesis and podocyte differentiation [45].

In *col4a1* fly mutants, we recorded severe myopathy, reduced concentration of COL4A1 protein [24], chronic inflammation, intestinal dysfunction [25], detachment of the cells from the BM by electron microscopy [26], compromised excretory system [27], heavy membrane peroxidation in epithelial cells of the Malpighian tubules [28] and the onset of muscular dystrophy in all mutants [29]. Temperature-sensitive *col4a1* alleles in *Drosophila* were generated by ethyl-methanesulfonate mutagenesis, resulting in G to A transitions in all alleles, in turn leading to glycine substitutions by Glu, Asp and Ser [29]. The phenotypic changes appeared in adult flies following 14 days of incubation at 29 °C and were not reversible, the flies did not recover at 20 °C following a shift in heat. We established the complementation map of the *col4a1-col4a2* locus with the aid of 34 mutants in all combinations in 561 independent crosses. The map was sharply divided into two non-overlapping parts with the dominant, temperature-sensitive alleles on one side, suggesting that only one of the two genes carries a temperature-sensitive mutation. Two mutant alleles of the same gene may restore the wild-type function in interallelic complementation [46]. We observed interallelic complementation among the temperature-sensitive *col4a1* alleles. This genetic observation indirectly suggests that at least two COL4A1 chains interact in forming the trimeric protomer, allowing the homotrimer $[COL4A1]_3$, $[COL4A2]_3$ or heterotrimer $[COL4A1]_2$COL4A2 composition of the triple helices [24]. In this paper, we present further phenotypic elements of the *col4a1* mutations, including Z-disc shifting to the level of M-discs, aberrant mitochondria in the epithelial cells of the Malpighian tubules and loss of sarcomere structure in the visceral muscles, providing further data of a BM-linked systemic condition.

2. Myopathic Defects in *Drosophila col4a1* Mutants

Under restrictive temperatures, the female heterozygotes become progressively more female-sterile [47]. We therefore chose the single-layer muscle fibers that encircle the common oviduct as a model. The system allowed the direct study of single muscle fibers and their sarcoplasmic membrane, without sectioning [24]. Muscle fibers in the *col4a1*^{G552D2} mutant detached laterally from each other and a thickened collagen IV-associated label appeared to fill the gap. The basement membrane covering the myofibers appeared distorted, thinned or absent, demonstrating that the mutant COL4A1 protein induced severe oviductal myopathy [24,26]. Integrin deposition in muscle fibers was recorded by punctate staining at the level of Z-discs, overlapping with the signals provided by the Z-disc protein kettin and bordering each sarcomeric unit in immunohistochemical preparation [29]. High expressivity of the trait occurred at low penetrance, i.e., shifting Z-disc integrin-binding sites toward the middle of sarcomeres in *col4a1*^{G552D1} mutants at the restrictive condition (Figure 1). The normal integrin-kettin staining still persisted at the level of the Z-discs and duplication of the Z-discs occurred at the level of M-discs (Figure 1, B4, B5, B6, white arrows). In some of the

replications this phenomenon occurred at nearly full expressivity; integrin staining was shifted quantitatively up to the level of M-discs, into the middle of the anisotropic band (Figure 1, C1, C2, C3, white arrows).

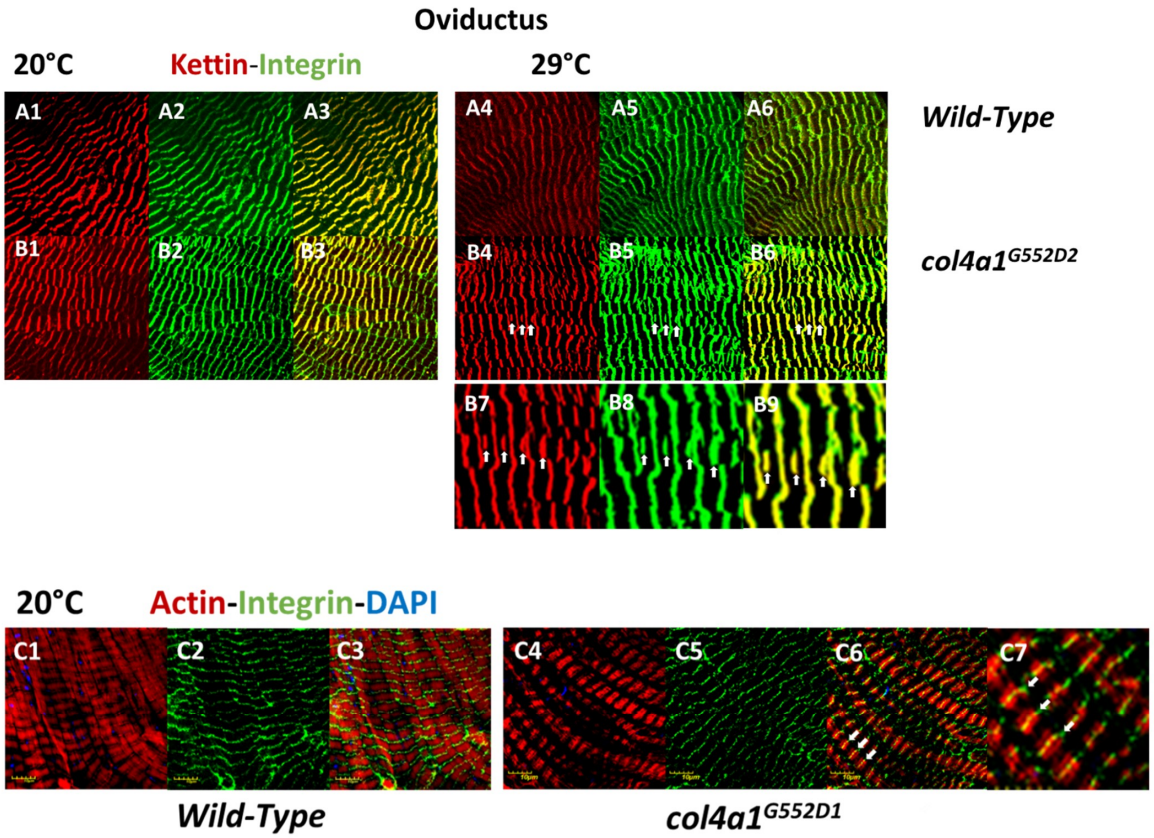

Figure 1. Shifting of Z-discs into the middle of sarcomeres, to the level of M-discs in striated muscle fibers of oviducts. The scaffold protein kettin is deposited at the level of the Z-discs (**A1**, **A4**, **B1**, **B4**) and overlaps with the integrin label (**A2**, **A5**, **B2**, **B5**) providing yellow-orange complementary colors in the overlays (**A3**, **A6**, **B3**, **B6**). Note the irregular integrin expression in the mutant at 29 °C, zig-zag pattern and streaming of Z-discs (**B5**). Additional kettin-integrin expression appears in the middle of sarcomeres at the level of M-discs (white arrows, **B4**, **B5**, **B6**). Higher magnification of areas in **B4**, **B5** and **B6** are marked by arrows (**B7**, **B8**, **B9**). The shifting of the integrin expression toward the middle of the sarcomeres is nearly at full expressivity (**C4**, **C5**, **C6**, white arrows). The area marked by arrows in C6 are at higher magnification (**C7**). Integrin expression remains at the sides of sarcomeres in Z-discs in the wild-type control (**C1**, **C2**, **C3**). Bars, lower left: 10 micrometers. Experiments were carried out as described [24–26,28,29].

Next, we quantitatively analyzed the phenomenon of Z-disc shifting in the wild-type control (*Oregon*) and *col4a1*^{G552D1} mutants and we labeled the level of expressivity by the Z-disc marker, kettin (Figure 2). The expressivity of Z-disc shifting occurred at over 8% in the wild-type control and over 12% in *col4a1*^{G552D2} mutants (Figure 2). We obtained the results by counting 6796 kettin-staining structures within the single-layer striated muscle of the common oviduct. Statistical analysis with the aid of the Welch two-sample t-test revealed significance at a value of $p = 0.003973$, indicating higher expressivity of the Z-disc shifting in the mutants (Figure 2).

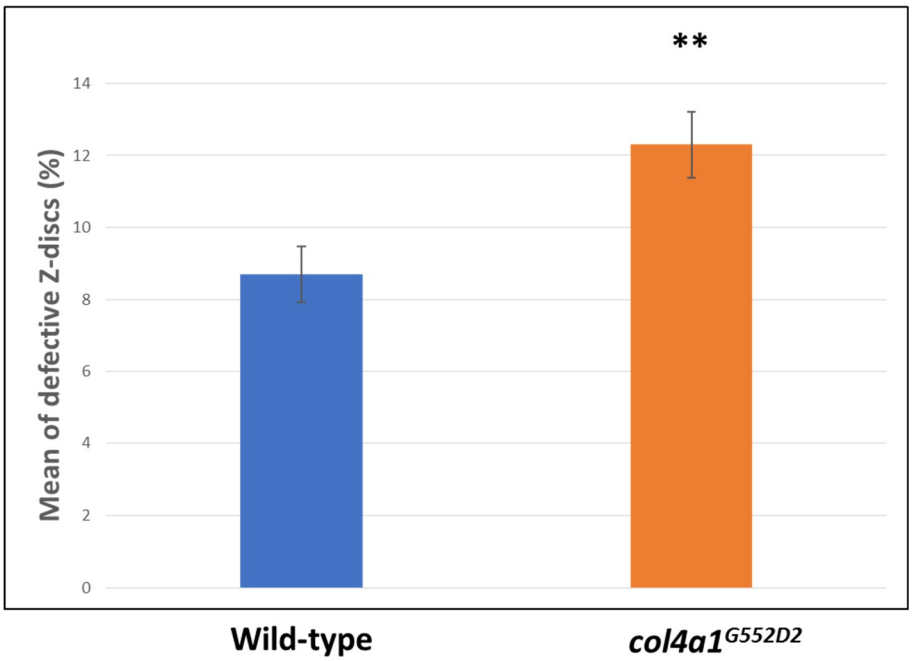

Figure 2. Elevated expressivity of Z-disc shifting in mutants. Statistically significant expressivity of Z-disc shifting in the mutants at $p = 0.003973$ (**).

3. Compromised Excretory System in the Mutants

Excretion is accomplished by the kidneys in vertebrates and by the Malpighian tubules in insects. As part of the clinical spectrum amino acid substitutions in the ubiquitous human BM component, COL4A1 can cause nephropathy. Affected patients develop renal dysfunction and chronic kidney failure with or without hematuria. Mouse *Col4a1* mutants present the same symptoms as humans. The Malpighian tubules are functionally similar to the mammalian kidneys and offer a versatile and tractable model [48]. The freely floating tubules are in continuous movement within the hemocoel, the blood-filled body cavity with open circulation. The mechanical load of periodic movements contributes to stress-induced cytoskeletal reorganization in *col4a1* mutant animals. We therefore tested the effects of mechanical load in the $col4a1^{G552D2}$ mutant and recorded the development of actin stress fibers and irregular, uneven actin staining in epithelial cells of the Malpighian tubules [27]. In a separate study, we noted mitochondrial fusion and co-localization of peroxynitrite-nitrated and 4-hydroxy-2-nonenal alkylated proteins with abnormal mitochondria [28]. Mitochondrial fusion in Malpighian epithelium is pronounced in the $col4a1^{G552D1}$ mutant at the restrictive temperature (Figure 3), as a sign of the mutation-induced stress, whereas the level of protein nitration assessed qualitatively remain unchanged in the wild-type control and mutant strains under both the permissive and restrictive conditions (Figure 3).

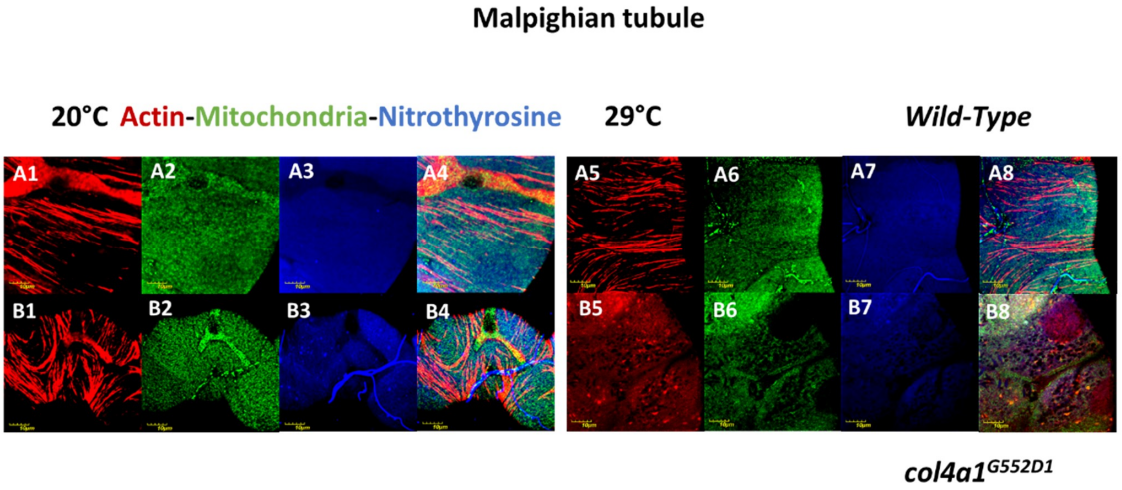

Figure 3. Compromised Malpighian tubules in mutants. Fusion and uneven distribution of mitochondria as a consequence of mutation-induced stress. Even distribution of mitochondria in wild-type control (**A1**, **A2**, **A3**, **A4**) and in the mutant under the permissive condition (**B1**, **B2**, **B3**, **B4**). The normal distribution of mitochondria remained at restrictive condition (**A5**, **A6**, **A7**, **A8**). Large aggregates of mitochondria appear in the mutant at 29 °C (**B5**, **B6**, **B7**, **B8**). Bars, lower left: 10 micrometers. Experiments were carried out as described [24–26,28,29].

4. Intestinal Manifestation of *col4a1* Mutations in *Drosophila*

The skeletal and cardiac muscles appeared 700 million years ago in a common ancestor prior to the evolutionary divergence of vertebrates and arthropods. The smooth muscle of vertebrates is likely to have evolved later, independent of the skeletal and cardiac muscle types [49]. Accordingly, the visceral muscles of *Drosophila* are striated. We studied the larval midgut through ultrathin sectioning and electron microscopy and observed that both epithelial and visceral muscle cells were severely degenerated at the restrictive temperature in $col4a1^{G552D2}$ mutant animals [26]. Both cell types detached from the distorted and thick BM, while epithelial cells accumulated lipid droplets, autophagic vacuoles and membrane ghosts. Membrane whorls practically filled the cell and the cytoplasm and muscle fibers were rarely observed. The space between the epithelial cell and the muscle cell was enlarged [26]. Functional damage of the alimentary tract in the $col4a1^{G552D2}$ mutant was reflected by intestinal dysfunction, degeneration of the gut epithelial cells recorded by terminal deoxynucleotidyl transferase dUTP nick end labeling (TUNEL) in the nuclei and the abrupt onset of leakiness of the gut (SMURF phenotype), demonstrated by blue food dye leaking out from the gut [25]. Intestinal dysfunction, a motility-associated disorder including chronic intestinal pseudo-obstruction, is a direct, life-threatening and frequent complication of muscular dystrophies, requiring immediate surgical intervention [50]. Notwithstanding, complications arising from intestinal dysfunction reported in *Drosophila col4a1* mutants in conjunction with *COL4A1* mutations have not yet been noted in humans and mice. We suggest that intestinal dysfunction in the $col4a1^{G552D2}$ mutant is a consequence of disrupted visceral muscle BM junction in the gut, without apparent sarcomere structure and amorphous, uneven actin deposition (Figure 4).

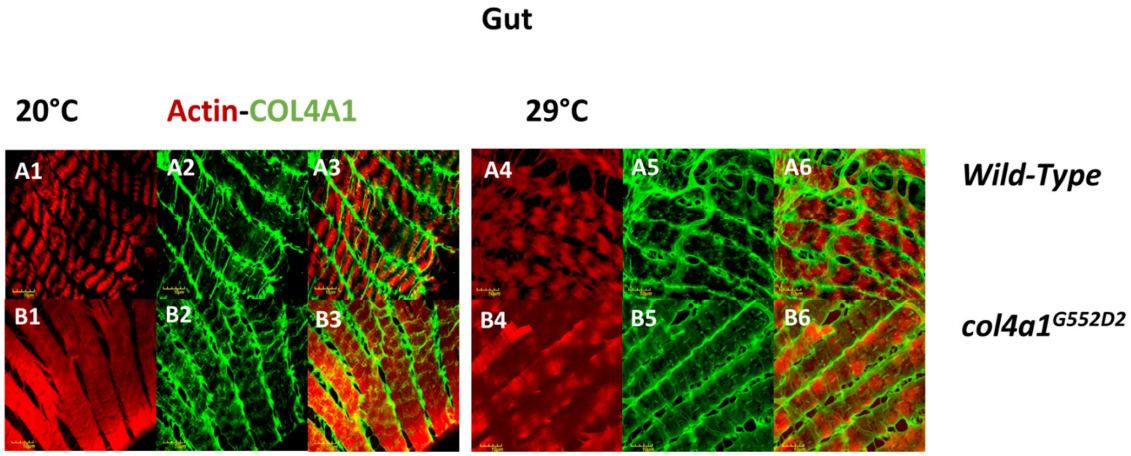

Figure 4. Loss of sarcomere structure in visceral muscle fibers. Regular sarcomere structure in the wild-type control at both temperatures (**A1**, **A2**, **A3** and **A4**, **A5**, **A6**) and loss of sarcomeres in the mutant that deposits actin in an irregular fashion (**B1**, **B2**, **B3** and **B4**, **B5**, **B6**). Bars, lower left: 10 micrometers. Experiments were carried out as described [24–26,28,29].

5. Materials and Methods

Wild-type *Oregon* flies and *col4a1* mutant lines were maintained at 20 °C and 29 °C on yeast-cornmeal-sucrose-agar food, consisting of nipagin to prevent fungal infection. The mutant stocks were kept heterozygous over the recombination—preventing *CyRoi* balancer chromosome. Malpighian tubules, common oviducts and the gut were dissected under carbon dioxide anesthesia from adults that were grown at either the permissive or the restrictive temperature for 14 days. Dissected organs were fixed in a previously prepared 4% paraformaldehyde dissolved in phosphate buffered saline (PBS) solution for 10 min, washed three times in PBS, permeabilized for 5 min in 0.1% Triton-X dissolved in PBS solution and washed three times in PBS. Blocking was achieved in a 5% bovine serum albumin dissolved in PBS solution for 1 h, and washed three times in PBS.

Complementation tests were performed by ethyl-methanesulfonate-induced point mutants, P-element insertional mutants and X-ray-generated deletion (null) alleles [24]. The mutation sites in eight temperature-sensitive lines were sequenced. All mutations were G to A transitions and replaced glycine with glutamate, aspartate and serine. The *a-30* allele carried the p.G233E amino acid substitution; the *b-9* carried the p.G467E substitution. The isoallelic lines *DTS-L2* and *DTS-L3* carried the p.G552D1 and p.G552D2 substitutions, respectively. The second isoallelic pair *DTS-L4* and *DTS-L5* carried the p.G1205E1 and p.G1205E2 substitutions, respectively, and the *DTS-L10* carried the p.G1043S substitution, whereas the *b-17* carried the p.G1393E substitution. Importantly, the lesions covered the collagenous domain of the COL4A1 protein [29].

Nuclei in the dissected organs were counter-stained by 1 µg/mL 4′,6-diamino-2-phenylindol (DAPI) in 20 µL PBS for 12 min in the dark. F-actin was stained by 1 unit Texas Red^{TM}-X Phalloidin (ThermoFisher) in 20 µL PBS for 20 min. Next, 1 µL mouse monoclonal anti-3-Nitrothyrosine, anti-integrin alpha PS and anti-kettin antibodies (Abcam) were used in 20 µL PBS for 1 h. Mouse anti-COL4A1 antibodies were raised by Creative Laboratory Ltd., Szeged, Hungary. Primary mouse antibodies were visualized by 1 µL F(ab') 2-Goat Anti-Mouse IgG (H+L) Cross Adsorbed Secondary Antibody conjugated with Alexa Fluor 488 (ThermoFisher) in 20 µL PBS for 1 h and 1 µL Goat Anti-Mouse IgG (H+L) Cross Adsorbed Secondary Antibody, Alexa Fluor 350, in 20 µL PBS for 1 h. Mitochondria were visualized by the mitochondrially targeted enhanced yellow fluorescent protein (mito-GFP) following appropriate crosses.

Photomicrographs were generated by confocal laser scanning fluorescence microscopy (Olympus Life Science Europa GmbH, Hamburg, Germany). The microscope configuration is described as follows. Objective lens: UPLSAPO 60× (oil, NA: 1.35); sampling speed: 8 µs/pixel; line averaging: 2×; scanning

mode: sequential unidirectional; excitation: 405 nm (DAPI), 543 nm (Texas Red) and 488 nm (Alexa Fluor 488); laser transmissivity: 7% was used for DAPI, 42% for Alexa Fluor 488 and 52% for Texas Red.

6. Conclusions

The basement membrane is likely to be the primordial form of the extracellular matrix and type IV collagen the key molecule in the transition from uni- to multicellularity [51]. The visco-elasticity of the BM is provided by the type IV collagen network, with defects in this component compromising the network's elasticity and function. Type IV collagen proteins are highly conserved structurally and functionally during evolution, including the mammalian–*Drosophila* relationship [51]. The ubiquitous human and mammalian BM consists of $(COL4A1)_2COL4A2$ heterotrimers and is distributed throughout the body. Glycine substitutions trigger systemic disease [1]. The genotype–phenotype relationship was established through 93 *COL4A1* and 12 *COL4A2* mutations. All of the lesions were dominant with nearly equal representation in males (48%) and females (52%). Inherited incidences were recorded at 47% and sporadic incidences at 53%. As observed in other types of collagens, triple helical Gly substitutions were the most prevalent class of mutations (68 out of 93 in *COL4A1*) and frequent substitutions were charged amino acids; Arg (30), Glu (11) and Asp (10) [52].

Expressivity of the *COL4A1* mutation-associated phenotypic elements often depends on genetic context in humans, mice and flies. In French families recapitulating key features of HANAC, different heterozygous missense mutations in the *COL4A1* gene were demonstrated [34]. In a Spanish family, tortuosity of the retinal arteries and retinal hemorrhage were identified, but the lesion was not associated with muscle cramps, renal or brain anomalies, although the p.G510R mutation was previously detected in a French family with HANAC syndrome [35]. Crossing of the *Col4a1* splice site mutant C57BL6/J mice with the 129/SvEvTac and CAST/EiJ inbred strains showed that the F1 progeny were phenotypically almost indistinguishable from the wild-type [42]. Similarly, in the isoallelic p.G552D1 and p.G552D2 mutants, the survival rates upon heat selection differed slightly. The line with the p.G552D1 lesion presented survival rates of 26.9% for pupae and 5.3% for adults, whereas the survival rates for the p.G552D2 line were 5.7% and 0.50%, respectively [24,29].

Here, we provided data on the systemic phenotype of the *col4a1* mutations and demonstrated the shifting of Z-discs, mitochondrial fusion and loss of sarcomeres in intestinal visceral muscle fibers. Genetic, genomic and proteomic data suggest that the fruit fly harbors all of the genetic elements of the BM, although the number of genes coding for BM components is apparently reduced in comparison with mammals, increasing the genetic tractability of the fly mutants' defective genes coding for proteins of the BM that are structurally and functionally conserved during evolution, including type IV collagens [53]. The dominant *col4a1* mutations therefore develop BM-specific phenotypes which are more severe than those observed in human and mouse models. Dominant temperature-sensitivity of the *col4a1* alleles is a lethal condition, which cannot be maintained in mammals. Nevertheless, the *col4a1*-associated phenotypic elements provide numerous biomarkers that can be measured quantitatively during the screening of large numbers of drugs in high-throughput *Drosophila* screens, aimed at alleviating symptoms of type IV collagenopathy.

Author Contributions: Conceptualization and methodology, M.M.; validation, A.A.K., N.S-P., M.M.; formal analysis, A.A.K., N.S-P., M.M.; resources, Z.B., V.T.; writing—original draft preparation, M.M., K.C., Z.B.; supervision and project administration, M.M.

Funding: This research was funded by the Hungarian Scientific Research Fund OTKA, grant number NN 108283 to M.M. and by the UNKP-18-3 New National Excellence Program of the Ministry of Human Capacities, grant number UNKP-18-3-IV-SZTE-23 to A.A.K. and UNKP-18-3-IV-SZTE-43 to N.S.-P.

Conflicts of Interest: The authors declare no conflict of interest.

References

1. Pozzi, A.; Yurchenco, P.D.; Iozzo, R.V. The nature and biology of basement membranes. *Matrix Biol.* **2017**, *57–58*, 1–11. [CrossRef]

2. Yurchenco, P.D.; Patton, B.L. Developmental and pathogenic mechanisms of basement membrane assembly. *Curr. Pharm. Des.* **2009**, *15*, 1277–1294. [CrossRef] [PubMed]
3. Sun, Z.; Guo, S.S.; Fässler, R. Integrin-mediated mechanotransduction. *J. Cell Biol.* **2016**, *215*, 445–456. [CrossRef] [PubMed]
4. Sado, Y.; Kagawa, M.; Naito, I.; Ueki, Y.; Seki, T.; Momota, R.; Oohashi, T.; Ninomiya, Y. Organization and expression of basement membrane collagen IV genes and their roles in human disorders. *J. Biochem.* **1998**, *123*, 767–776. [CrossRef]
5. Kashtan, C.E. Alport syndrome. An inherited disorder of renal, ocular, and cochlear basement membranes. *Medicine (Baltimore)* **1999**, *78*, 338–360. [CrossRef] [PubMed]
6. Miosge, N. The ultrastructural composition of basement membranes in vivo. *Histol. Histopathol.* **2001**, *16*, 1239–1248. [PubMed]
7. Jimenez-Mallebrera, C.; Brown, S.C.; Sewry, C.A.; Muntoni, F. Congenital muscular dystrophy: molecular and cellular aspects. *Cell. Mol. Life Sci.* **2005**, *62*, 809–823. [CrossRef]
8. Kanagawa, M.; Toda, T. The genetic and molecular basis of muscular dystrophy: roles of cell-matrix linkage in the pathogenesis. *J. Hum. Genet.* **2006**, *51*, 915–926. [CrossRef]
9. Matejas, V.; Hinkes, B.; Alkandari, F.; Al-Gazali, L.; Annexstad, E.; Aytac, M.B.; Barrow, M.; Bláhová, K.; Bockenhauer, D.; Cheong, H.I.; et al. Mutations in the human laminin beta2 (LAMB2) gene and the associated phenotypic spectrum. *Hum. Mutat.* **2010**, *31*, 992–1002. [CrossRef]
10. Alport, A.C. Hereditary Familial Congenital Haemorrhagic Nephritis. *Br. Med. J.* **1927**, *1*, 504–506. [CrossRef]
11. Pihlajaniemi, T.; Tryggvason, K.; Myers, J.C.; Kurkinen, M.; Lebo, R.; Cheung, M.C.; Prockop, D.J.; Boyd, C.D. cDNA clones coding for the pro-alpha1(IV) chain of human type IV procollagen reveal an unusual homology of amino acid sequences in two halves of the carboxyl-terminal domain. *J. Biol. Chem.* **1985**, *260*, 7681–7687.
12. Boyd, C.D.; Weliky, K.; Toth-Fejel, S.; Deak, S.B.; Christiano, A.M.; Mackenzie, J.W.; Sandell, L.J.; Tryggvason, K.; Magenis, E. The single copy gene coding for human alpha 1 (IV) procollagen is located at the terminal end of the long arm of chromosome 13. *Hum. Genet.* **1986**, *74*, 121–125. [CrossRef]
13. Brazel, D.; Pollner, R.; Oberbäumer, I.; Kühn, K. Human basement membrane collagen (type IV). The amino acid sequence of the alpha 2(IV) chain and its comparison with the alpha 1(IV) chain reveals deletions in the alpha 1(IV) chain. *Eur. J. Biochem.* **1988**, *172*, 35–42. [CrossRef]
14. Butkowski, R.J.; Langeveld, J.P.; Wieslander, J.; Hamilton, J.; Hudson, B.G. Localization of the Goodpasture epitope to a novel chain of basement membrane collagen. *J. Biol. Chem.* **1987**, *262*, 7874–7877.
15. Saus, J.; Wieslander, J.; Langeveld, J.P.; Quinones, S.; Hudson, B.G. Identification of the Goodpasture antigen as the alpha 3(IV) chain of collagen IV. *J. Biol. Chem.* **1988**, *263*, 13374–13380.
16. Hostikka, S.L.; Eddy, R.L.; Byers, M.G.; Höyhtyä, M.; Shows, T.B.; Tryggvason, K. Identification of a distinct type IV collagen alpha chain with restricted kidney distribution and assignment of its gene to the locus of X chromosome-linked Alport syndrome. *Proc. Natl. Acad. Sci. USA* **1990**, *87*, 1606–1610. [CrossRef]
17. Oohashi, T.; Sugimoto, M.; Mattei, M.G.; Ninomiya, Y. Identification of a new collagen IV chain, alpha 6(IV), by cDNA isolation and assignment of the gene to chromosome Xq22, which is the same locus for COL4A5. *J. Biol. Chem.* **1994**, *269*, 7520–7526.
18. Antignac, C.; Zhou, J.; Sanak, M.; Cochat, P.; Roussel, B.; Deschênes, G.; Gros, F.; Knebelmann, B.; Hors-Cayla, M.C.; Tryggvason, K. Alport syndrome and diffuse leiomyomatosis: deletions in the 5′ end of the COL4A5 collagen gene. *Kidney Int.* **1992**, *42*, 1178–1183. [CrossRef]
19. Antignac, C.; Knebelmann, B.; Drouot, L.; Gros, F.; Deschênes, G.; Hors-Cayla, M.C.; Zhou, J.; Tryggvason, K.; Grünfeld, J.P.; Broyer, M. Deletions in the COL4A5 collagen gene in X-linked Alport syndrome. Characterization of the pathological transcripts in nonrenal cells and correlation with disease expression. *J. Clin. Investig.* **1994**, *93*, 1195–1207. [CrossRef]
20. Lemmink, H.H.; Mochizuki, T.; van den Heuvel, L.P.; Schröder, C.H.; Barrientos, A.; Monnens, L.A.; van Oost, B.A.; Brunner, H.G.; Reeders, S.T.; Smeets, H.J. Mutations in the type IV collagen alpha 3 (COL4A3) gene in autosomal recessive Alport syndrome. *Hum. Mol. Genet.* **1994**, *3*, 1269–1273. [CrossRef]
21. Lemmink, H.H.; Schröder, C.H.; Monnens, L.A.; Smeets, H.J. The clinical spectrum of type IV collagen mutations. *Hum. Mutat.* **1997**, *9*, 477–499. [CrossRef]
22. Kalluri, R.; Shield, C.F.; Todd, P.; Hudson, B.G.; Neilson, E.G. Isoform switching of type IV collagen is developmentally arrested in X-linked Alport syndrome leading to increased susceptibility of renal basement membranes to endoproteolysis. *J. Clin. Investig.* **1997**, *99*, 2470–2478. [CrossRef]

23. Hudson, B.G.; Tryggvason, K.; Sundaramoorthy, M.; Neilson, E.G. Alport's Syndrome, Goodpasture's Syndrome, and Type IV Collagen. *N. Engl. J. Med.* **2003**, *348*, 2543–2556. [CrossRef]
24. Kelemen-Valkony, I.; Kiss, M.; Csiha, J.; Kiss, A.; Bircher, U.; Szidonya, J.; Maróy, P.; Juhász, G.; Komonyi, O.; Csiszár, K.; et al. Drosophila basement membrane collagen col4a1 mutations cause severe myopathy. *Matrix Biol.* **2012**, *31*, 29–37. [CrossRef]
25. Kiss, M.; Kiss, A.A.; Radics, M.; Popovics, N.; Hermesz, E.; Csiszár, K.; Mink, M. Drosophila type IV collagen mutation associates with immune system activation and intestinal dysfunction. *Matrix Biol.* **2016**, *49*, 120–131. [CrossRef]
26. Kelemen-Valkony, I.; Kiss, M.; Csiszar, K.; Mink, M. Inherited Myopathies. In *Myopathies: New Research*; Washington, H.S., Jimenez, C.E.C., Eds.; Nova Science Publishers: Hauppauge, NY, USA, 2012; ISBN 9781622573721.
27. Kiss, A.A.; Popovics, N.; Szabó, G.; Csiszár, K.; Mink, M. Altered stress fibers and integrin expression in the Malpighian epithelium of Drosophila type IV collagen mutants. *Data Brief* **2016**, *7*, 868–872. [CrossRef]
28. Kiss, A.A.; Popovics, N.; Boldogkői, Z.; Csiszár, K.; Mink, M. 4-Hydroxy-2-nonenal Alkylated and Peroxynitrite Nitrated Proteins Localize to the Fused Mitochondria in Malpighian Epithelial Cells of Type IV Collagen Drosophila Mutants. *BioMed Res. Int.* **2018**, *2018*, 3502401. [CrossRef]
29. Kiss, A.A.; Popovics, N.; Marton, K.; Boldogkoi, Z.; Csiszar, K.; Mink, M. Type IV collagen is essential for proper function of integrin-mediated adhesion in Drosophila muscle fibers. *bioRxiv* **2018**, 318337. [CrossRef]
30. Smit, L.M.; Barth, P.G.; Valk, J.; Njiokiktjien, C. Familial porencephalic white matter disease in two generations. *Brain Dev.* **1984**, *6*, 54–58. [CrossRef]
31. Aguglia, U.; Gambardella, A.; Breedveld, G.J.; Oliveri, R.L.; Le Piane, E.; Messina, D.; Quattrone, A.; Heutink, P. Suggestive evidence for linkage to chromosome 13qter for autosomal dominant type 1 porencephaly. *Neurology* **2004**, *62*, 1613–1615. [CrossRef]
32. Gould, D.B.; Phalan, F.C.; Breedveld, G.J.; van Mil, S.E.; Smith, R.S.; Schimenti, J.C.; Aguglia, U.; van der Knaap, M.S.; Heutink, P.; John, S.W.M. Mutations in Col4a1 Cause Perinatal Cerebral Hemorrhage and Porencephaly. *Science (80-.)* **2005**, *308*, 1167–1171. [CrossRef]
33. Plaisier, E.; Gribouval, O.; Alamowitch, S.; Mougenot, B.; Prost, C.; Verpont, M.C.; Marro, B.; Desmettre, T.; Cohen, S.Y.; Roullet, E.; et al. *COL4A1* Mutations and Hereditary Angiopathy, Nephropathy, Aneurysms, and Muscle Cramps. *N. Engl. J. Med.* **2007**, *357*, 2687–2695. [CrossRef]
34. Plaisier, E.; Chen, Z.; Gekeler, F.; Benhassine, S.; Dahan, K.; Marro, B.; Alamowitch, S.; Paques, M.; Ronco, P. Novel COL4A1 mutations associated with HANAC syndrome: a role for the triple helical CB3[IV] domain. *Am. J. Med. Genet. A* **2010**, *152A*, 2550–2555. [CrossRef]
35. Zenteno, J.C.; Crespí, J.; Buentello-Volante, B.; Buil, J.A.; Bassaganyas, F.; Vela-Segarra, J.I.; Diaz-Cascajosa, J.; Marieges, M.T. Next generation sequencing uncovers a missense mutation in COL4A1 as the cause of familial retinal arteriolar tortuosity. *Graefe's Arch. Clin. Exp. Ophthalmol.* **2014**, *252*, 1789–1794. [CrossRef]
36. Weng, Y.-C.; Sonni, A.; Labelle-Dumais, C.; de Leau, M.; Kauffman, W.B.; Jeanne, M.; Biffi, A.; Greenberg, S.M.; Rosand, J.; Gould, D.B. COL4A1 mutations in patients with sporadic late-onset intracerebral hemorrhage. *Ann. Neurol.* **2012**, *71*, 470–477. [CrossRef]
37. Yoneda, Y.; Haginoya, K.; Kato, M.; Osaka, H.; Yokochi, K.; Arai, H.; Kakita, A.; Yamamoto, T.; Otsuki, Y.; Shimizu, S.; et al. Phenotypic Spectrum of *COL4A1* Mutations: Porencephaly to Schizencephaly. *Ann. Neurol.* **2013**, *73*, 48–57. [CrossRef]
38. Abe, Y.; Matsuduka, A.; Okanari, K.; Miyahara, H.; Kato, M.; Miyatake, S.; Saitsu, H.; Matsumoto, N.; Tomoki, M.; Ihara, K. A severe pulmonary complication in a patient with COL4A1-related disorder: A case report. *Eur. J. Med. Genet.* **2017**, *60*, 169–171. [CrossRef]
39. Meuwissen, M.E.C.; Halley, D.J.J.; Smit, L.S.; Lequin, M.H.; Cobben, J.M.; de Coo, R.; van Harssel, J.; Sallevelt, S.; Woldringh, G.; van der Knaap, M.S.; et al. The expanding phenotype of COL4A1 and COL4A2 mutations: clinical data on 13 newly identified families and a review of the literature. *Genet. Med.* **2015**, *17*, 843–853. [CrossRef]
40. Labelle-Dumais, C.; Dilworth, D.J.; Harrington, E.P.; de Leau, M.; Lyons, D.; Kabaeva, Z.; Manzini, M.C.; Dobyns, W.B.; Walsh, C.A.; Michele, D.E.; et al. COL4A1 Mutations Cause Ocular Dysgenesis, Neuronal Localization Defects, and Myopathy in Mice and Walker-Warburg Syndrome in Humans. *PLoS Genet.* **2011**, *7*, e1002062. [CrossRef]

41. Van Agtmael, T.; Schlötzer-Schrehardt, U.; McKie, L.; Brownstein, D.G.; Lee, A.W.; Cross, S.H.; Sado, Y.; Mullins, J.J.; Pöschl, E.; Jackson, I.J. Dominant mutations of Col4a1 result in basement membrane defects which lead to anterior segment dysgenesis and glomerulopathy. *Hum. Mol. Genet.* **2005**, *14*, 3161–3168. [CrossRef]
42. Gould, D.B.; Marchant, J.K.; Savinova, O.V.; Smith, R.S.; John, S.W.M. Col4a1 mutation causes endoplasmic reticulum stress and genetically modifiable ocular dysgenesis. *Hum. Mol. Genet.* **2007**, *16*, 798–807. [CrossRef]
43. Guiraud, S.; Migeon, T.; Ferry, A.; Chen, Z.; Ouchelouche, S.; Verpont, M.-C.; Sado, Y.; Allamand, V.; Ronco, P.; Plaisier, E. HANAC Col4a1 Mutation in Mice Leads to Skeletal Muscle Alterations due to a Primary Vascular Defect. *Am. J. Pathol.* **2017**, *187*, 505–516. [CrossRef]
44. Kuo, D.S.; Labelle-Dumais, C.; Mao, M.; Jeanne, M.; Kauffman, W.B.; Allen, J.; Favor, J.; Gould, D.B. Allelic heterogeneity contributes to variability in ocular dysgenesis, myopathy and brain malformations caused by Col4a1 and Col4a2 mutations. *Hum. Mol. Genet.* **2014**, *23*, 1709–1722. [CrossRef]
45. Chen, Z.; Migeon, T.; Verpont, M.-C.; Zaidan, M.; Sado, Y.; Kerjaschki, D.; Ronco, P.; Plaisier, E. HANAC Syndrome Col4a1 Mutation Causes Neonate Glomerular Hyperpermeability and Adult Glomerulocystic Kidney Disease. *J. Am. Soc. Nephrol.* **2016**, *27*, 1042–1054. [CrossRef]
46. Clifford, R.; Schüpbach, T. Molecular analysis of the Drosophila EGF receptor homolog reveals that several genetically defined classes of alleles cluster in subdomains of the receptor protein. *Genetics* **1994**, *137*, 531–550.
47. Suzuki, D.T.; Procunier, D. Temperature-sensitive mutations in Drosophila melanogaster. 3. Dominant lethals and semilethals on chromosome 2. *Proc. Natl. Acad. Sci. USA* **1969**, *62*, 369–376. [CrossRef]
48. Dow, J.A.T.; Romero, M.F. *Drosophila* provides rapid modeling of renal development, function, and disease. *Am. J. Physiol.* **2010**, *299*, F1237–F1244. [CrossRef]
49. OOta, S.; Saitou, N. Phylogenetic relationship of muscle tissues deduced from superimposition of gene trees. *Mol. Biol. Evol.* **1999**, *16*, 856–867. [CrossRef]
50. Connor, F.L.; Di Lorenzo, C. Chronic Intestinal Pseudo-obstruction: Assessment and Management. *Gastroenterology* **2006**, *130*, S29–S36. [CrossRef]
51. Fidler, A.L.; Darris, C.E.; Chetyrkin, S.V.; Pedchenko, V.K.; Boudko, S.P.; Brown, K.L.; Gray Jerome, W.; Hudson, J.K.; Rokas, A.; Hudson, B.G. Collagen IV and basement membrane at the evolutionary dawn of metazoan tissues. *eLife* **2017**, *6*, e24176. [CrossRef]
52. Jeanne, M.; Gould, D.B. Genotype-phenotype correlations in pathology caused by collagen type IV alpha 1 and 2 mutations. *Matrix Biol.* **2016**. [CrossRef]
53. Ramos-Lewis, W.; Page-McCaw, A. Basement membrane mechanics shape development: Lessons from the fly. *Matrix Biol.* **2018**. [CrossRef]